2011 Water Reactor Fuel Performance Meeting
Chengdu, China, Sept. 11-14, 2011
T3-031

CLADDING HYDROGEN BASED REGULATIONS IN THE UNITED STATES

Patrick A.C. Raynaud and Andrew S. Bielen
United States Nuclear Regulatory Commission, Washington, DC, 20555, USA
patrick.raynaud@nrc.gov

Abstract: To take into account the effect of burnup and hydrogen on fuel performance during Loss-Of-Coolant Accidents (LOCAs) and Reactivity Initiated Accidents (RIAs), the United States Nuclear Regulatory Commission (USNRC) is currently considering implementing several hydrogen based regulations. The proposed new LOCA criterion and the interim RIA criterion are characterized by hydrogen or corrosion dependent safety limits. As a result, it is foreseen that analysis tools will be needed that take into account hydrogen in order to show compliance with the new criteria and the associated new rules.
The NRC has hydrogen pickup models for Zircaloy-2 cladding under boiling water reactor (BWR) conditions and for Zircaloy-4, ZIRLO™, and M5™ cladding under pressurized water reactor (PWR) conditions. These models were used to determine representative hydrogen levels and distribution in nuclear fuel rods during operation. This information was combined with the proposed 10 CFR 50.46(b) LOCA acceptance criteria, and with the USNRC Standard Review Plan Section 4.2 (NUREG-0800) interim RIA acceptance criterion to derive allowable equivalent cladding reacted (ECR) and fuel enthalpy rise, respectively, as a function of burnup and axial location.
These results demonstrate a reasonable method of implementing hydrogen-based limits to govern cladding behavior during design basis accidents. In doing so, the analyses demonstrate how hydrogen in the cladding can be used as a surrogate for burnup effects.

Keywords: LOCA; RIA; hydrogen; regulation.

1. INTRODUCTION

The US Nuclear Regulatory Commission (NRC) is in the process of revising both the Emergency Core Cooling System (ECCS) acceptance criteria (10 CFR 50.46(b) [1]) and the Reactivity Initiated Accident (RIA) acceptance criteria (NUREG-0800, Chapter 4.2, Appendix B [2]) to take into account the degradation in fuel cladding mechanical properties with radiation and temperature exposure in a nuclear reactor environment. Specifically, for the new proposed ECCS criteria, the allowable Equivalent Cladding Reacted (ECR) – a measure of how much high-temperature oxidation is acceptable locally on a fuel rod during a Loss of Coolant Accident (LOCA) – will decrease as a function of pre-transient hydrogen concentration in the cladding. Similarly, for the proposed RIA fuel cladding failure criteria, the allowable fuel enthalpy rise (ΔH) – a measure of how much energy can be deposited in the fuel without causing failure – will decrease as a function of pre-transient hydrogen concentration in the cladding for Boiling Water Reactors (BWR) and as a function of the ratio of oxide to cladding thickness for Pressurized Water Reactors (PWR). This is in contrast to the current criteria, which for allow 17% local ECR and 280 cal/g peak radial average fuel enthalpy respectively, regardless of the burnup or hydrogen content.

Because the new LOCA and RIA criteria are to be hydrogen or corrosion dependent, it is important to consider the differences between BWRs and PWRs, particularly in terms of the operational differences and the use of different cladding alloys having different corrosion and hydrogen pickup properties. Historically, Zircaloy-2 has been used in BWRs and Zircaloy-4 has been used in PWRs. However, as the demands on fuel have increased over the years because of extensive power uprates and higher discharge burnups, new cladding alloys have been developed and deployed across the U.S. PWR fleet. The two "advanced" PWR cladding products currently in widespread use are the Westinghouse product ZIRLO™, and the AREVA product M5™. Overall, it can be said that evolutionary changes in the chemistry and processing of these two modern alloys have resulted in greater corrosion resistance when compared to Zircaloy-4.

The first objective of the current study was to use the FRAPCON-3.4a steady-state fuel behavior code [3] to provide information on the relationship between rod burnup and cladding degradation in terms of hydrogen pickup for the four cladding alloys used in U.S. nuclear reactors. For BWR cladding (modern Zircaloy-2 variants), the hydrogen pickup model in FRAPCON-3.4a is only dependent on burnup, thus this relationship is independent of the rod temperature history. On the other hand, for PWR cladding alloys, it is well-established that the hydrogen concentration in the fuel rod cladding is a strong function of the manner in which the rod is operated. In fact, two rods with equivalent burnup may have different hydrogen contents depending on the power and temperature history of each rod.

In other words, a rod that is operated at a high linear heat generation rate with a corresponding higher cladding temperature will have higher hydrogen content than a rod that is operated at a lower linear heat generation rate for the same rod average burnup. The FRAPCON-3.4a PWR cladding hydrogen pickup models consider these variables, and thus a one-to-one relationship between hydrogen and burnup does not exist. Since the new ECR and fuel enthalpy rise limits are stated as a function of hydrogen content, it was desirable to correlate the hydrogen concentration as a function of rod burnup to investigate the burnup dependence of the LOCA and RIA criteria.

The second objective of this study was to use the relationship established between hydrogen content and burnup to generate burnup dependent allowable ECR and fuel enthalpy rise limits for the four cladding alloys used in U.S. nuclear reactors. For each cladding alloy, the LOCA and RIA limits were generated not only as a function of burnup but also axial position in the core (axial node), to fully capture the hydrogen dependence of the allowable ECR [4] and fuel enthalpy rise [2], which decrease with cladding degradation over the operational lifetime of the fuel assembly. Finally, the burnup dependent LOCA and RIA limits were compared as a function of cladding alloy for the axial node with the highest hydrogen pickup. It should be noted that this comparison assumed identical power histories for the three PWR cladding alloys (based on the operation of a reactor using ZIRLO™ cladding). This assumption was deemed necessary to be able to compare the FRAPCON-3.4a models for hydrogen pickup on a common basis for a given type of reactor.

2. TYPICAL FUEL PERFORMANCE MODELING

The NRC steady-state fuel performance code FRAPCON-3.4a was used to model fuel cladding performance over the lifetime of a fuel assembly for a representative GE BWR/4 reactor and a representative of a 4-loop Westinghouse (W4LP) PWR. The BWR/4 and W4LP reactors modeled are part of the U.S. fleet and will be designated as reactor B and P, respectively, for BWR and PWR.

The cladding material used in reactor B is modern Zircaloy-2, while ZIRLO™ is used in the P reactor. Typical BWR 10x10 and PWR 17x17 fuel geometries were used for the B and P reactor, respectively. The thermal-hydraulic boundary conditions, power histories and axial and radial power distributions were extracted from the proprietary Updated Final Safety Analysis Report (UFSAR) and the Fuel Cycle Design Report for reactors B and P. A typical arrangement of fresh, once-burned, and twice burned fuel assemblies is shown in Figure 1 for the B and P reactors. The conditions used as inputs for the fuel behavior code are representative of an average BWR and PWR, respectively. These conditions serve as a guideline for the way in which a reactor core would operate, but it is well established that each cycle is somewhat unique in its loading pattern and operating characteristics. Furthermore, every nuclear reactor is different and should be analyzed with its actual design parameters.[1]

A detailed reactor physics calculation would provide exact values of burnup as a function of assembly life. For the purposes of this study, however, approximations were used to estimate the operating histories of typical assemblies within the reactor core. Specifically, it was assumed that if an assembly operates at relatively high power throughout the first cycle of its life, then it will operate at a somewhat lower power later in life. Conversely, an assembly that operates at relatively lower power early in its life will then be operated at higher power in its second or third cycle in the core.

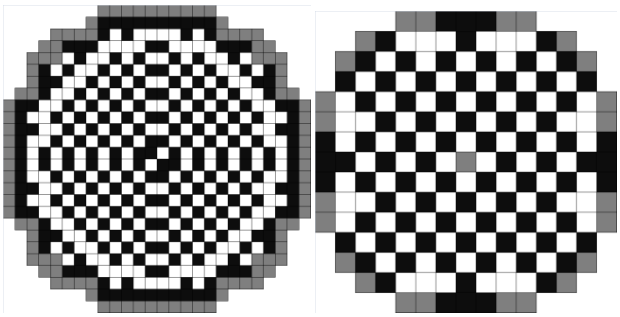

Figure 1: Typical BWR/4 and 4-loop PWR core load patterns used for FRAPCON calculations (white: fresh assembly, black: once burned, gray: twice burned).

The information required to generate rod power histories was obtained from the UFSAR and the Fuel Cycle Design Report for the B and P reactors. Table 1 and Table 2 present the FRAPCON 3.4a inputs used for rod average linear heat generation rate (LHGR) as a function of cycle, assembly power level bin, and time in cycle. The power levels chosen were based on relative average assembly powers as a function of time in cycle. The LHGR values for points in between beginning of cycle (BOC) and middle of cycle (MOC), and in between MOC and end of cycle (EOC), were interpolated. The core average LHGR was 15.99 kW/m for the B reactor and 18.99 kW/m for the P reactor. It is recognized that there is some intra-assembly power gradient, so that not every rod experiences the assembly-average LHGR throughout the assembly life. However, the purpose of this exercise was to obtain representative values for particular rod design parameters, and thus the detailed behavior of individual hot or cold rods within an assembly are not taken into account here.

For modeling purposes in FRAPCON-3.4a, the fuel rod was divided into 12 foot-long axial nodes. The core axial power distribution was assumed identical for every assembly, but it did change with time throughout the cycle. The available information only permitted the modeling of three axial profiles for the P reactor, corresponding to BOC, MOC and EOC. In contrast, more detailed axial profile information was available for the B reactor, and 16 different

[1] The generic cases presented here are only to be taken as examples of how fuel behavior codes can be used to derive burnup dependent LOCA and RIA criteria, and should not be applied directly in support of licensing.

axial profiles were modeled for a given cycle.

Table 1: BWR inputs for the rod average linear heat generation rates for each cycle and power level.

	Core average LHGR (kW/m)			15.99
Cycle	Power	Rod Average LHGR (kW/m)		
		BOC	MOC	EOC
1	High	20.52	17.78	21.22
	Mid	17.24	15.74	18.47
	Low	16.41	14.33	16.94
2	High	17.42	15.96	17.94
	Mid-High	17.45	14.46	15.35
	Mid-Low	15.24	12.70	13.35
	Low	13.11	10.62	10.95
3	High	12.89	9.84	10.49
	Mid-High	10.06	9.00	7.39
	Mid-Low	8.94	6.97	6.86
	Low	7.61	5.90	5.66

Table 2: PWR inputs for the rod average linear heat generation rates for each cycle and power level.

	Core average LHGR (kW/m)			18.99
Cycle	Power	Rod Average LHGR (kW/m)		
		BOC	MOC	EOC
1	High	25.54	25.66	24.21
	Mid	23.59	24.76	23.68
	Low	19.50	18.72	19.86
2	High	22.81	23.91	23.23
	Mid-High	21.93	20.55	20.79
	Mid-Low	19.88	19.81	19.24
	Low	11.05	11.15	12.19
3	Mid	19.45	19.52	19.01
	Low	10.08	9.82	11.07

Two cycle and three cycle assembly lifetimes were considered. Consequently, a large number of combinations can be generated based on the above power bins for each type of reactor. Only realistic power histories were retained, such that the maximum rod average burnup limit of 62 GWd/MTU (the current regulatory limit in the U.S.) at the end of its life was not exceeded. In addition, only rod average discharge burnups above 45 GWd/MTU for the P reactor, and between 40 and 50 GWd/MTU for the B reactor, were retained. The elimination process resulted in 7 possible power histories for the P reactor, and 18 for the B reactor.

It should be acknowledged here that the power histories employed in this study for the P reactor are based on the use of ZIRLO™ cladding. Thus, they are not necessarily appropriate or representative of a plant that continues to use Zircaloy-4, or that has switched to M5™. As mentioned above, due to more demanding operating strategies (such as power uprate conditions and/or extended burnup), many power plants have needed to switch to advanced cladding alloys in order to demonstrate that their fuel integrity under these conditions would be maintained. It is not necessarily representative of Zircaloy-4 or M5™ to simulate their behavior when submitted to power histories from a plant using ZIRLO™ cladding. However, for the purposes of this demonstration, and to highlight the performance of Zircaloy-4 relative to the more advanced alloys ZIRLO™ and M5™, the same power histories were used for all three PWR cladding alloys.

3. HYDROGEN CONTENT PREDICTIONS

The non-proprietary corrosion and hydrogen pickup models employed in FRAPCON 3.4a are alloy-specific, and can be found in the FRAPCON 3.4a description document [3]. For all PWR alloys, the corrosion layer is modeled as a metal-oxide interface temperature-dependent cubic rate law until a transition thickness is reached. At that point, a neutron flux dependent linear rate law is applied, with the rate constant being an Arrhenius function of oxide-metal interface temperature. The transition thickness and activation energies can be different depending on the specific alloy in question. Post-irradiation examination indicates that Zircaloy-4 accumulates a corrosion layer much faster than either M5™ or ZIRLO™ for an equivalent flux and temperature history. This difference is predicted by the FRAPCON-3.4a models. For Zircaloy-2 under boiling-water reactor (BWR) conditions, a flux-dependent linear rate law is applied, with the rate constant being an Arrhenius function of oxide-metal interface temperature. For all four alloys, since the corrosion layer has a reduced thermal conductivity relative to the base metal, and corrosion growth rate is proportional to oxide-metal interface temperature, the thicker the oxide layer is, the faster corrosion will build up. In this way, corrosion growth exhibits some positive feedback characteristics.

In addition to its relatively poor cladding corrosion behavior, Zircaloy-4 cladding also exhibits greater hydrogen pickup relative to M5™ and ZIRLO™. For the PWR alloys, FRAPCON3.4a models hydrogen pickup as a constant fraction of the hydrogen generated in the corrosion reaction, whereby M5™ has a pickup fraction of 0.10, ZIRLO™ has a pickup fraction of 0.125, and Zircaloy-4 has a pickup fraction of 0.15. Thus, for a given corrosion rate, a higher proportion of produced hydrogen is absorbed into Zircaloy-4 than the other alloys. Coupled with the fact that the corrosion growth rate is much higher for Zircaloy-4 relative to the other alloys, it can be seen that one would expect a much higher corrosion thickness and hydrogen content for calculations using Zircaloy-4 instead of the more advanced alloys. In contrast, the Zircaloy-2 hydrogen pickup model is not dependent on the corrosion rate, but is instead entirely dependent on burnup [3][5]. Consequently, for burnups up to about 50 GWd/MTU, the hydrogen content of Zircaloy-2 is relative low when compared to the PWR alloys. Above this burnup level, hydrogen pickup increases rapidly due its exponential dependence on burnup:

$$[H]_{Zircaloy\text{-}2} = 22.8 + \exp(0.117 \times (BU - 20))$$

Figure 2 through Figure 5 show the FRAPCON-3.4a results for hydrogen concentration as a function of burnup for each of the alloys and rod histories investigated. For the sake of clarity, only seven of the twelve fuel rod nodes modeled are shown. Node 1 corresponds with the bottom of the fuel rod, and Node 12 corresponds with the top of the fuel rod.

For Zircaloy-2, as can be seen in Figure 2, since the

hydrogen pickup model only depends on burnup, the hydrogen content versus burnup plots for all nodes and operating histories lie exactly on the same line. This results from the way hydrogen pickup is modeled in FRAPCON-3.4a.

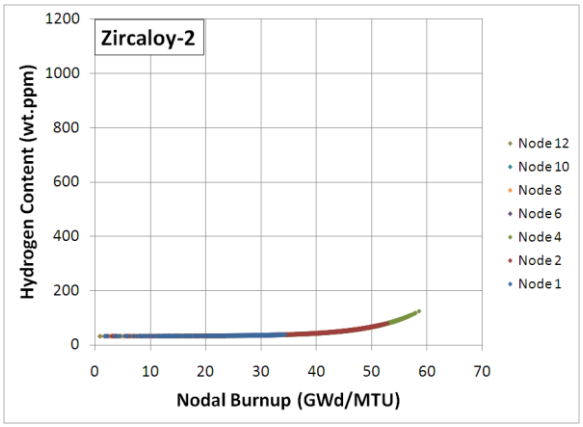

Figure 2: Axial node distribution of hydrogen versus burnup for Zircaloy-2 cladding and typical BWR power histories.

For the PWR cladding alloys Zircaloy-4 (Figure 3) and ZIRLO™ (Figure 4), a considerable spread exists in the possible hydrogen content at equivalent burnup, even for a given axial elevation. This variability indicates that the hydrogen content in the cladding indeed depends upon the particular operating history followed. Furthermore, hydrogen contents vary with axial location. This variation results from the direct dependence of hydriding on corrosion, which is a temperature dependent phenomenon. In fact, it can be seen that the hydrogen content dependence on temperature (i.e. axial location) is larger than the dependence on rod power history, as is particularly visible for higher burnups, where axial variations are very large.

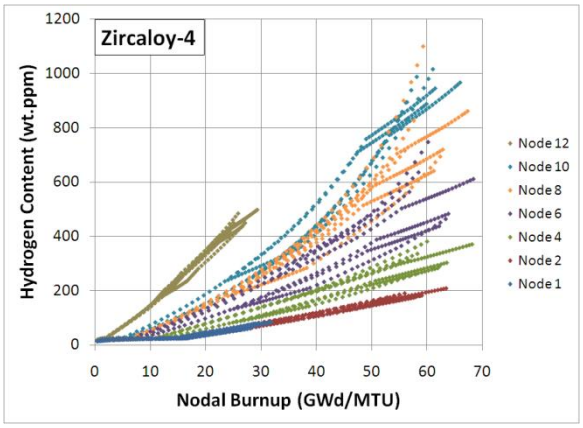

Figure 3: Axial node distribution of hydrogen versus burnup for Zircaloy-4 cladding and typical PWR power histories.

The very high hydrogen contents observed for Zircaloy-4 in Figure 3 for burnups greater than 40 GWd/MTU are correlated with thick oxide layers. It is worth noting that vendors have fuel rod design-related acceptance criteria by which once a certain corrosion layer is reached, the fuel cannot be operated anymore. In Figure 3, the hydrogen contents above 650 wt.ppm correspond to oxide thicknesses that would be excessive in most vendor analyses, and thus may not be representative of what would actually be observed in a reactor core being operated with Zircaloy-4 cladding. However, as mentioned above, the same power histories were assumed for all three PWR cladding alloys for comparison purposes.

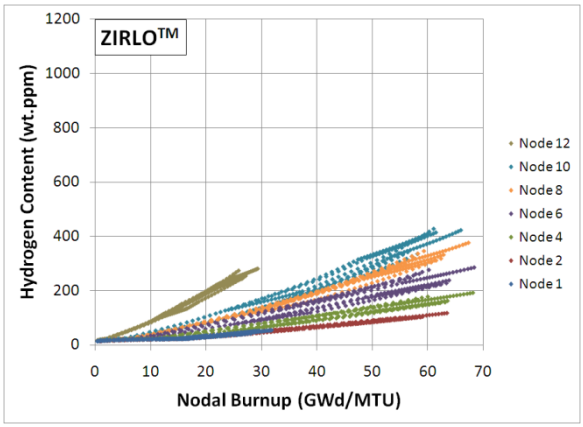

Figure 4: Axial node distribution of hydrogen versus burnup for ZIRLO™ cladding and typical PWR power histories.

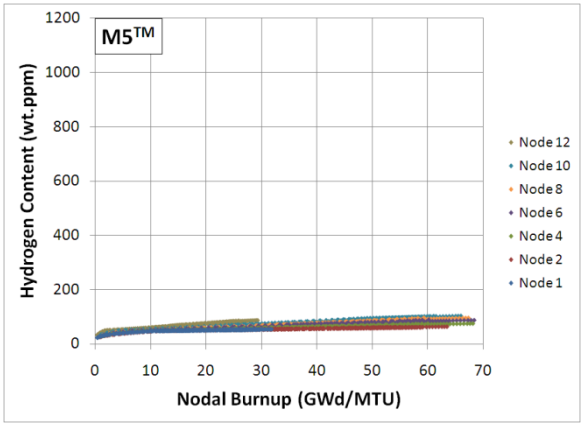

Figure 5: Axial node distribution of hydrogen versus burnup for M5™ cladding and typical PWR power histories.

As is particularly noticeable in Figure 3 and Figure 4, the behaviors of Node 1 and Node 12 further emphasize the temperature dependence of the corrosion rate equation, and thus hydrogen content. The axial power distributions employed in this analysis are fairly flat across a given cycle, with the top and bottom nodes experiencing roughly half the accumulated fluence (and thus burnup) as the rest of the rod. Since Node 1 is at the bottom of the core, and has the coolest cladding temperature, it accumulates relatively little hydrogen. Node 12, on the other hand, is still at an elevated temperature due to its location at the top of the core, and accumulates significant amounts of hydrogen. Thus, for equivalent nodal burnups, one can clearly see very strong temperature dependence in hydrogen pickup behavior in Zircaloy-4.

The positive feedback in oxide layer thickness and cladding-oxide interface temperature may also be evident in this plot, for some power histories run on Nodes 8, 9 and 10. As the oxide layer grows thicker, the conductance of heat out of the cladding deteriorates, driving the oxide-metal interface temperature up. This causes the corrosion reaction to accelerate, creating even more oxide, and thus hydrogen

pickup. Thus, for high burnups, the corrosion layer and corresponding hydrogen content can be quite high.

The M5™ alloy, shown in Figure 5, has a flatter hydrogen content versus burnup profile when compared to Zircaloy-4 and ZIRLO™. The very low hydrogen contents observed in M5™ are a result of the fact that the transition in corrosion kinetics (and thus hydrogen pickup) has not yet occurred in this alloy for peak nodal burnups close to 70 GWd/MTU and for the power histories assumed in this study. If a sufficient oxide layer thickness was reached, trends similar to those observed in Zircaloy-4 and ZIRLO™ would be expected for M5™.

As expected, for all three PWR cladding alloys, the location of peak hydrogen concentration is consistent with the location of maximum corrosion. This is because hydrogen pickup is modeled as a simple function of local corrosion [3], and thus the highest hydrogen concentration exists at the location of the maximum corrosion. Within each individual fuel operating cycle, it is evident that the predicted burnup and corrosion behavior is higher for fuel that is run at higher LHGR than those run at lower LHGR. The maximum fuel centerline and average temperatures reach their maximum values high up in the core, where the heat flux is still relatively high and the coolant temperatures outside the rod are also high, reducing the heat transfer and raising the fuel temperatures of that node.

4. BURNUP DEPENDENT LOCA LIMITS

The new proposed ECR limits that constitute one of the ECCS acceptance criteria takes into account fuel cladding degradation over core lifetime, and decreases with hydrogen content [H] according to the following relationships [4]:

It should be noted that, due to the limitations of the current database, the proposed criterion only considers hydrogen contents below 600 wt.ppm, at which point the allowable ECR drops to zero; however, for the purpose of this study, it was assumed that the relationship valid above 400 wt.ppm was valid beyond hydrogen contents of 600 wt.ppm.

The burnup dependent hydrogen contents calculated with FRAPCON 3.4a for the four different cladding alloys in use in the U.S. fleet, and described in the previous section, were used as inputs to the hydrogen dependent ECR limit equations. In doing so, it was possible to plot allowable ECR as a function of burnup for every axial node and power history simulated for each alloy. Figure 6 through Figure 9 show the allowable ECR (dependent on axial level and power history) as a function of burnup.

For Zircaloy-2, as can be seen on Figure 6, the allowable ECR as a function of burnup lies on the same line for all axial nodes and all power histories. This lack of variation can be explained by the fact that the hydrogen pickup model for Zircaloy-2 in FRAPCON-3.4a only depends on burnup. Additionally, since the hydrogen content remains low for Zircaloy-2 cladding in a BWR environment and burnups below 50 GWd/MTU, the apparent performance of this alloy in terms of the ECR limit is quite good. In fact, according to the FRAPCON-3.4a model, the allowable ECR at 60 GWd/MTU is close to 14%, which is still a significant fraction of the 18% limit proposed for fresh cladding. It should, however, be pointed out that the exponential increase in hydrogen content that occurs rapidly beyond 50 GWd/MTU would result in a very rapid performance degradation at higher burnups.

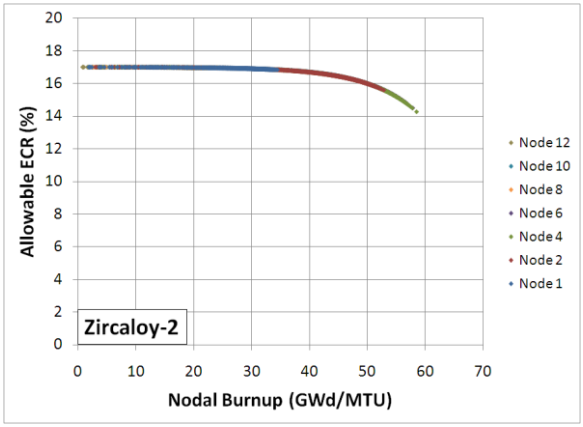

Figure 6: Axial node allowable ECR as a function of burnup for Zircaloy-2 cladding and typical BWR power histories.

For the PWR alloys Zircaloy-4 and ZIRLO™ shown in Figure 7 and Figure 8, the allowable ECR decreases significantly with burnup, especially for Zircaloy-4 and for nodes in the upper half of the core. The extreme case is for Zircaloy-4 cladding at Node 10, where one power history resulted in an end-of-life allowable ECR equal to zero. The hydrogen content that corresponds with this point is close to 1100 wt.ppm, and the corrosion layer thickness is nearly 130 microns. This is a result of the power histories chosen for this study, and it is possible but not likely that a fuel rod would be loaded into a position in the core where it would be predicted to accumulate so much oxide. Therefore, this rod history may not be representative of the actual operating characteristics of a PWR that still uses Zircaloy-4 cladding. For M5™, shown in Figure 9, the decrease in allowable ECR predicted with FRAPCON-3.4a is not as sharp as for the two other PWR alloys. This can be explained by the fact that the oxide thickness has not reached the transition point at which oxidation rate, and thus hydrogen pickup rate, increase rapidly.

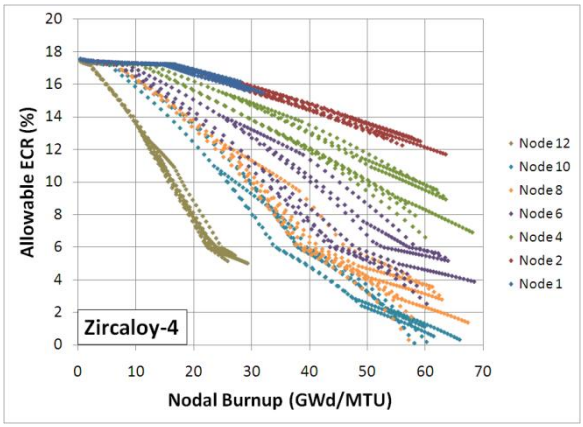

Figure 7: Axial node allowable ECR as a function of burnup for Zircaloy-4 cladding and typical PWR power histories.

Another observation is that in some cases (particularly in the top half of the core) there is a considerable spread in the allowable ECR for a given burnup: up to ~5% for a given node and 12% between nodes. This is due to the differences in power histories as well as axial coolant temperature distribution, resulting in differences in metal-oxide layer interface temperature distribution for each of the cases calculated. As expected based on the predictions of hydrogen content presented above, the impact of axial position in the core on acceptable ECR is larger than the impact of the different power histories.

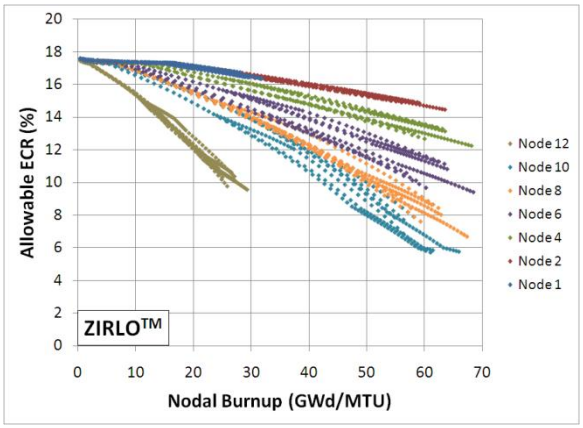

Figure 8: Axial node allowable ECR as a function of burnup for ZIRLO™ cladding and typical PWR power histories.

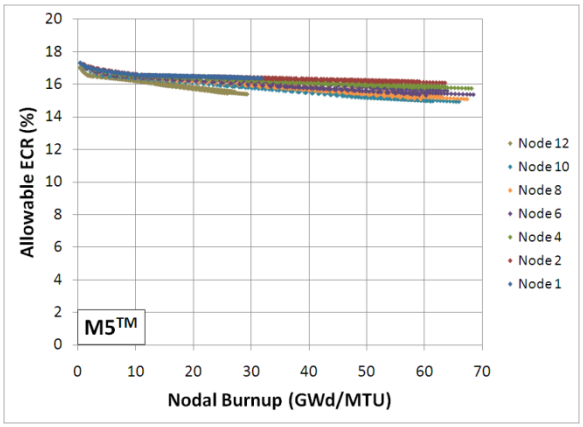

Figure 9: Axial node allowable ECR as a function of burnup for M5™ cladding and typical PWR power histories.

The difference between allowable ECR versus burnup for Zircaloy-2, Zircaloy-4, ZIRLO™, and M5™ is shown in Figure 10. The calculation results shown correspond to the highest hydrogen content node at assembly end of life.

As mentioned above, Zircaloy-2 appears to perform better than the other alloy with regards to the ECR limit for burnups up to 55 GWd/MTU. However, the Zircaloy-2 hydrogen pickup model increases exponentially with burnup in FRAPCON-3.4a, so the code predictions are such that the allowable ECR would drop rapidly beyond 60 GWd/MTU and would be equal to zero at 79 GWd/MTU.

For PWR cladding alloys, one can compare the allowable ECR curves generated with FRAPCON-3.4a for Zircaloy-4, where the maximum predicted hydrogen concentration was 1100 wt.ppm, with those obtained for ZIRLO™ and M5™, where the maximum predicted hydrogen concentration were 450 wt.ppm and 105 wt.ppm respectively. This comparison shows that Zircaloy-4 has significantly lower allowable ECR values at high burnups than more advanced cladding alloys such as ZIRLO™ or M5™. Consequently, depending on both the operating characteristics of the reactor and the assumptions made in the LOCA analysis, some Zircaloy-4 plants may have more difficulty meeting the proposed 10 CFR 50.46(b) ECCS acceptance criteria ECR limit than those using more advanced cladding alloys such as ZIRLO™ or M5™. Again, it is acknowledged that the power histories used in the calculations presented in this report may not be fully representative of what is in use in the operating fleet. The resulting allowable ECR as a function of burnup documented in this report may thus be conservatively low. This study could be improved with plant-specific operating histories should one want a more precise prediction of the allowable ECR values as a function of burnup.

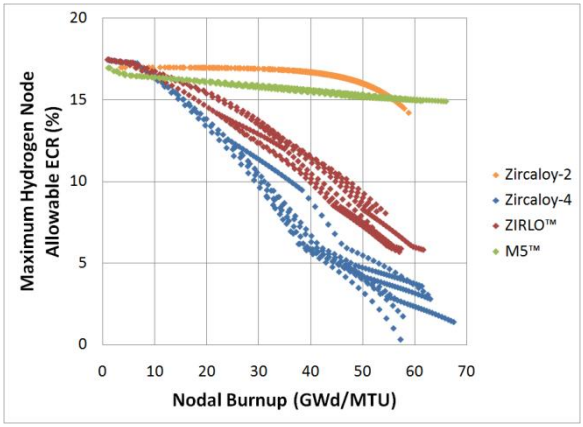

Figure 10: Comparison of allowable ECR versus burnup between Zircaloy-2 (BWR), Zircaloy-4 (PWR), ZIRLO™ (PWR), and M5™ (PWR). The axial node shown corresponds to maximum cladding hydrogen content.

5. BURNUP DEPENDENT RIA LIMITS

As is the case for the ECR limit in the ECCS criteria, the new proposed fuel enthalpy rise limit that constitute the pellet-cladding mechanical interaction portion of the RIA acceptance criteria takes into account fuel cladding degradation over core lifetime. In the interim criteria described in NUREG-0800 [2], the allowable fuel enthalpy rise ΔH decreases with hydrogen content [H] for BWRs and with oxide to wall thickness ratio δ_O/t for PWRs. The following relationships describe the fuel enthalpy rise limits.

For PWRs:

$\Delta H_{allowable} = 150$ $\delta_O/t < 0.04$

$\Delta H_{allowable} = 225 - 1825 \times \delta_O/t$ $0.04 < \delta_O/t < 0.08$

$\Delta H_{allowable} = 85 - 125 \times \delta_O/t$ $0.08 < \delta_O/t$

For BWRs:

$\Delta H_{allowable} = 150$ $[H] < 75$

$\Delta H_{allowable} = 240 - 1.2 \times [H]$ $75 < [H] < 150$

$\Delta H_{allowable} = 70 - 2/30 \times [H]$ $150 < [H]$

It should be noted that because of current limitations in the experimental database, the proposed criteria only consider oxide to wall thickness ratios below 0.2 and hydrogen contents below 300 wt.ppm, at which points the

allowable fuel enthalpy rise drops to zero. However, for the purpose of this study, it was assumed that the relationships valid above $\delta_O/t = 0.08$ and [H] = 150 wt.ppm were valid beyond $\delta_O/t = 0.2$ and [H] = 300 wt.ppm.

The burnup dependent hydrogen contents calculated with FRAPCON 3.4a for Zircaloy-2 were used as inputs to the hydrogen dependent allowable fuel enthalpy rise equations. In doing so, it was possible to plot allowable fuel enthalpy rise as a function of burnup for every axial node and power history simulated for Zircaloy-2, as shown in Figure 11. For Zircaloy-2, according to the hydrogen pickup model in FRAPCON-3.4a, the threshold of 75 wt.ppm for constant allowable fuel enthalpy rise is reached for a burnup of about 52 GWd/MTU. As a result, the allowable fuel enthalpy rise is equal to 150 cal/g up to a burnup of 52 GWd/MTU, but then drops sharply as the hydrogen content increases exponentially.

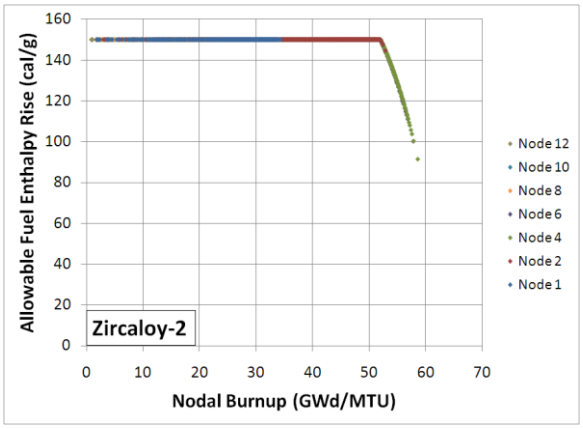

Figure 11: Axial node allowable fuel enthalpy rise as a function of burnup for Zircaloy-2 cladding and typical BWR power histories.

For the PWR cladding alloys Zircaloy-4, ZIRLO™, and M5™, the FRAPCON-3.4a predicted oxide thickness was divided by the cladding wall thickness and used as input for the PWR allowable fuel enthalpy rise criterion. The allowable fuel enthalpy rise as a function of burnup for Zircaloy-4, ZIRLO™, and M5™ for all the power histories and axial locations modeled are shown in Figure 12, Figure 13, and Figure 14 respectively.

As can be observed in Figure 12 and Figure 13, once the threshold corresponding to a ratio of oxide to wall thickness of 0.04 is reached, the allowable fuel enthalpy rise decreases rapidly from 150 cal/g to 75 cal/g. Below 75 cal/g, corresponding to oxide to wall thickness ratio of 0.08, the rate of decrease in allowable fuel enthalpy rise is much slower, in accordance with the equations describing the criterion. As was the case for the ECR limit, there is considerable spread in the allowable fuel enthalpy rise for a given burnup: up to ~60cal/g for a given node and ~80cal/g between nodes. Once again, this spread is due to the differences in power histories as well as axial coolant temperature distribution. In addition, the impact of axial position in the core on acceptable fuel enthalpy rise is again larger than the impact of the different power histories, albeit to a lesser extent than was the case for ECR. It should be noted that although the proposed LOCA and RIA limits are expressed in terms of local maxima, the analysis of a LOCA is global (system wide) in nature while the analysis of RIA energy insertion is local in nature. That is, the peak fuel enthalpy rise in the RIA event occurs at high axial locations in the core, which also happens to be the place where the corrosion levels are highest.

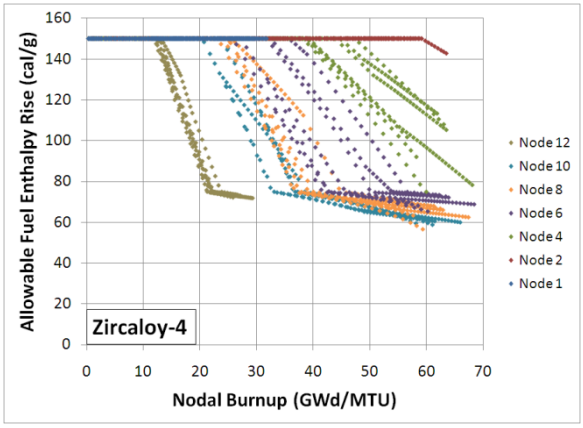

Figure 12: Axial node allowable fuel enthalpy rise as a function of burnup for Zircaloy-4 cladding and typical PWR power histories.

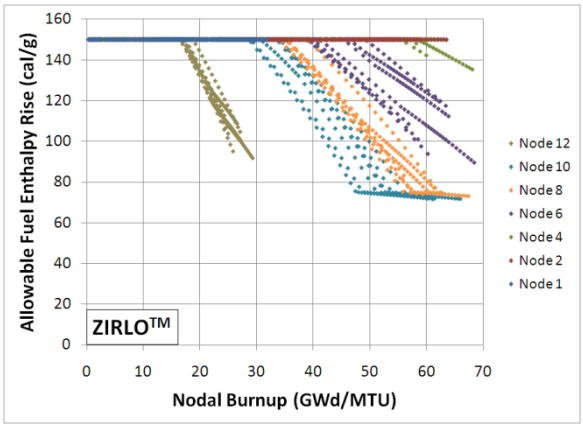

Figure 13: Axial node allowable fuel enthalpy rise as a function of burnup for ZIRLO™ cladding and typical PWR power histories.

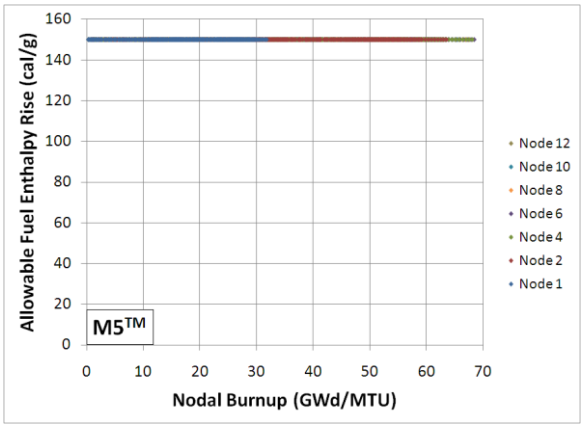

Figure 14: Axial node allowable fuel enthalpy rise as a function of burnup for M5™ cladding and typical PWR power histories.

In contrast to Zircaloy-4 and ZIRLO™, the M5™ alloy does not undergo a transition in oxidation rate for the power

histories modeled in this study, because the oxide layer is significantly thinner than for the other two PWR cladding alloys. In fact, the oxide thickness corresponding to an oxide to cladding wall thickness ratio of 0.04 is never predicted, thus the allowable fuel enthalpy rise remains constant at 150 cal/g, as can be observed in Figure 14.

Figure 15 illustrates the differences in behavior for the four alloys investigated and the set of power histories modeled in this study. The calculation results shown correspond to the highest hydrogen content node at assembly end of life.

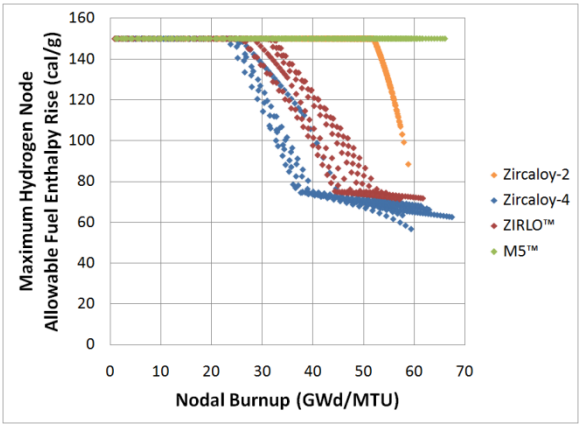

Figure 15: Comparison of allowable fuel enthalpy rise versus burnup between Zircaloy-2 (BWR), Zircaloy-4 (PWR), ZIRLO™ (PWR), and M5™ (PWR). The axial node shown corresponds to maximum cladding hydrogen content.

Zircaloy-2 appears to perform better than Zircaloy-4 and ZIRLO™ with regards to the fuel enthalpy rise limit for burnups up to 60 GWd/MTU. However, the Zircaloy-2 hydrogen pickup model increases exponentially with burnup in FRAPCON-3.4a, so the code predictions are such that the allowable fuel enthalpy rise would be equal to zero at 80 GWd/MTU. Coincidentally, although there is no theoretical relationship between allowable ECR and fuel enthalpy rise, it is interesting to note that, for Zircaloy-2, the predicted zero allowable ECR occurs at 79 GWd/MTU.

For PWR cladding alloys, the FRAPCON-3.4a predictions are such that the oxide thickness for M5™ never becomes large enough for the transition in corrosion rate to occur. A consequence of the superior corrosion behavior of M5™ compared to Zircaloy-4 and ZIRLO™ is that the oxide to cladding thickness ratio remains below 0.04, and the allowable fuel enthalpy rise remains constant at 150 cal/g. When comparing Zircaloy-4 and ZIRLO™, it can be said that the end-of-life allowable fuel enthalpy rise is relatively similar (within 20 cal/g), but the reactors using Zircaloy-4 will be limited to a fuel enthalpy rise below 80 cal/g earlier in core life: around 35 GWd/MTU for Zircaloy-4 versus 45 GWd/MTU for ZIRLO™.

Consequently, according to the FRAPCON-3.4a models developed in this study, and depending on both the operating characteristics of the reactor and the assumptions made in the RIA analysis, Zircaloy-4 and ZIRLO™ plants will be challenged earlier in their RIA analysis than plants using M5™. It should be acknowledged here once again that the power histories used in the calculations presented in this report may not be fully representative of what is in use in the operating fleet, particularly for Zircaloy-4 and M5™, so the above conclusions should only be treated as a case study, and are not necessarily representative of the reality in the U.S. PWR fleet. This study could be improved with plant-specific operating histories should one want a more precise prediction of the allowable fuel enthalpy rise values as a function of burnup.

6. CONCLUSIONS

The first objective of this study was to investigate the relationship between rod burnup and cladding degradation primarily in terms of hydrogen content, but also oxide thickness, for a typical PWR and BWR of the U.S. fleet. A method was developed to generate characteristic power histories based on information gathered from the UFSAR and Fuel Cycle Design Reports from a BWR/4 using modern Zircaloy-2 as its fuel cladding, and a Westinghouse 4-loop PWR using ZIRLO™ as its fuel cladding. It was shown that:

1. For Zircaloy-2 in a BWR environment, the FRAPCON-3.4a models for hydrogen pickup are entirely dependent on burnup.
2. For Zircaloy-4, ZIRLO™, and M5™ in a PWR environment, the relationship between hydrogen and burnup is dependent on power history and axial position in the core.
3. For PWR environments, the axial position in the core has a larger impact than the power history of the rod on predicted hydrogen content as a function of burnup.

The second objective of this study was to generate burnup dependent ECR and fuel enthalpy rise limits (part of the ECCS and RIA acceptance criteria, respectively) for Zircaloy-2, Zircaloy-4, ZIRLO™, and M5™. The relationships between hydrogen and burnup generated using FRAPCON-3.4a for all four cladding alloys investigated were used as inputs to the ECR and fuel enthalpy rise limits described in the proposed LOCA and RIA criteria to be implemented in the near future. These criteria take into account the deleterious effects of hydrogen and corrosion on transient cladding performance. With the assumptions made in this study, it was shown that:

1. For identical power histories, , PWRs using Zircaloy-4 will be challenged earlier than plants using more modern alloys such as ZIRLO™ or M5™.
2. Within the assumptions of this study and the potential limitations of FRAPCON-3.4a, Zircaloy-2 behaved well compared to the PWR alloys until a certain burnup level was reached, typically 50-55 GWd/MTU, at which point the exponential increase in hydrogen content caused the ECR and fuel enthalpy rise limits to decrease very rapidly.
3. If burnup were to be extended beyond 65 or 70 GWd/MTU, the performance of Zircaloy-2 in BWRs would be worse than for ZIRLO™ and M5™ in PWRs, and the predicted limits would become equal to zero around 78-80 GWd/MTU.

In summary, this study is useful in understanding the impact of power histories and axial location within the core on the FRAPCON-3.4a predictions of ECR and fuel enthalpy rise limits, which constitute part of the ECCS and RIA acceptance criteria, respectively. However, it is important to recognize that some of the assumptions made for the purposes of this modeling study may not reflect actual industry practices, and thus plant-specific information should be used to produce case-by-case allowable limits.

REFERENCES

[1]. Nuclear Regulatory Commission, 13 August 2009, Federal Register, Vol. 74, no. 155, pp. 40765-40776.
[2]. Nuclear Regulatory Commission, 2007, NUREG-0800, Ch. 4.2, Rev. 3, pp. 33-36.
[3]. Geelhood, K.J., et al., 2011, NUREG/CR-7022.
[4]. Nuclear Regulatory Commission, 2010, Draft Generic Letter, ADAMS Accession Number ML100960505.
[5]. Geelhood, K.J., et al., 2009, NUREG/CR-7001.